

Identification of senescence-associated circular RNAs (SAC-RNAs) reveals senescence suppressor *CircPVT1*

Amaresh C. Panda^{*,†}, Ioannis Grammatikakis^{*,†}, Kyoung Mi Kim, Supriyo De, Jennifer L. Martindale, Rachel Munk, Xiaoling Yang, Kotb Abdelmohsen and Myriam Gorospe

Laboratory of Genetics and Genomics, National Institute on Aging, Intramural Research Program, National Institutes of Health, Baltimore, MD 21224, USA

Received August 04, 2016; Revised October 25, 2016; Editorial Decision November 14, 2016; Accepted November 18, 2016

ABSTRACT

Using RNA sequencing (RNA-Seq), we compared the expression patterns of circular RNAs in proliferating (early-passage) and senescent (late-passage) human diploid WI-38 fibroblasts. Among the differentially expressed senescence-associated circRNAs (which we termed ‘SAC-RNAs’), we identified *CircPVT1*, generated by circularization of an exon of the *PVT1* gene, as a circular RNA showing markedly reduced levels in senescent fibroblasts. Reducing *CircPVT1* levels in proliferating fibroblasts triggered senescence, as determined by a rise in senescence-associated β -galactosidase activity, higher abundance of CDKN1A/P21 and TP53, and reduced cell proliferation. Although several microRNAs were predicted to bind *CircPVT1*, only let-7 was found enriched after pulldown of endogenous *CircPVT1*, suggesting that *CircPVT1* might selectively modulate let-7 activity and hence expression of let-7-regulated mRNAs. Reporter analysis revealed that *CircPVT1* decreased the cellular pool of available let-7, and antagonizing endogenous let-7 triggered cell proliferation. Importantly, silencing *CircPVT1* promoted cell senescence and reversed the proliferative phenotype observed after let-7 function was impaired. Consequently, the levels of several proliferative proteins that prevent senescence, such as IGF2BP1, KRAS and HMGA2, encoded by let-7 target mRNAs, were reduced by silencing *CircPVT1*. Our findings indicate that the SAC-RNA *CircPVT1*, elevated in dividing cells and reduced in senescent cells, sequesters let-7 to enable a proliferative phenotype.

INTRODUCTION

Cellular senescence is a state of indefinite growth arrest triggered by exposure of cell to stress-causing stimuli (1). It was first described by Hayflick in 1965 and has been studied extensively in cultured cells (2). When the stress signal arises from successive rounds of replication causing gradual shortening of telomeres, which exposes telomeric DNA and triggers a DNA damage response, the ensuing program is named *replicative senescence* (3–6). When the stress signal comes from other sources of damage, such as oxidants, radiation, heat, activated oncogenes, or toxins, the ensuing program is named *stress-induced senescence* (6–9). Senescence is characterized by increased activity of the tumor suppressor TP53, higher levels of its transcriptional target p21/CDKN1 and the CDK inhibitor p16/INK4A, and activation of the p16 target retinoblastoma (pRB) (7,8). Senescent cells have a complex impact on human physiology and pathology. Some effects of senescent cells are beneficial, such as tissue remodeling, wound repair, and growth suppression of potentially oncogenic cells (10). However, many effects of senescent cells are believed to be detrimental. Besides causing tissue dysfunction, senescent cells exhibit a senescence-associated secretory phenotype (SASP), whereby they produce and secrete inflammatory cytokines and chemokines, matrix metalloproteases, and growth and angiogenic factors (11). The accumulation of senescent cells has been associated with disease processes such as sarcopenia, arthritis, cancer, diabetes, and neurodegeneration (12–14).

MicroRNAs (miRNAs) are ~22-nucleotide long non-coding (nc)RNAs that form part of the RNA-induced silencing complex (RISC), within which the RNA-binding protein (RBP) AGO2 binds microRNAs directly. MicroRNA–RISC complexes influence protein expression patterns through the interaction of the microRNA with subsets of mRNAs via partial complementarity, generally leading to reduced stability and/or reduced translation of the mRNA (15). By influencing protein expression patterns,

To whom correspondence should be addressed. Tel: +1 410 558 8240; Fax: +1 410 558 8331; Email: amaresh.panda@nih.gov

Correspondence may also be addressed to Ioannis Grammatikakis. Tel: +1 410 558 8606; Fax: +1 410 558 8331; Email: yannis.grammatikakis@nih.gov

[†]These authors contributed equally to this work as first authors.

microRNAs have been implicated in key cellular processes, including proliferation, survival, differentiation, immune activation, stress response, and cell senescence. As reviewed recently, microRNAs impact upon numerous pathways that control senescence (16). Indeed, many microRNAs show altered expression levels during senescence (17,18).

A notable class of microRNAs implicated in growth arrest and senescence is the human let-7 family, which consists of 13 different microRNAs with homology to the *Caenorhabditis elegans* let-7, a regulator of development and aging (19–24). Given that let-7 members are expressed from genomic regions that are deleted in tumors and that they suppress expression of oncogenes and proteins that enhance cell proliferation, the let-7 family has been implicated in tumor suppression (20,25,26). Accordingly, let-7 levels are reduced in many malignancies, including cancers of the lung, prostate, ovarian, breast, and thyroid (27–31). Conversely, let-7 members have been proposed to promote senescence, as their levels rise during cell senescence and let-7 suppresses the production of proteins that promote proliferation and inhibit senescence (17,32,33). One let-7 target, HMGA2 (high-mobility group AT-hook 2), promotes mesenchymal tumorigenesis, and suppresses cellular senescence (34–39). Other let-7 targets include oncoproteins in the Ras family, specifically NRAS, KRAS and HRAS, which contain let-7 binding sequences in their 3'-untranslated regions (UTRs) (40). Low let-7 levels permit high RAS expression and thus let-7 microRNAs have been proposed to suppress proliferation (40); in the case of KRAS, let-7 suppresses translation without changing *KRAS* mRNA levels (41). Another target, the IGF2BP1 (insulin growth factor 2 mRNA-binding protein 1; also known as IMP1), is highly expressed during embryogenesis and in various tumors; let-7 is suggested to regulate its expression by targeting the 3'UTR of the *IGF2BP1* mRNA (42,43).

Circular RNAs (circRNAs) are ncRNAs that form covalently closed circles. Initially, they were considered byproducts of splicing, but recent work has revealed that a vast number of circRNAs exist in mammalian cells and that some of them are abundant and stable, suggesting that they may have regulatory functions in the cell. RNA circularization is mainly accomplished through the process of back-splicing (44), whereby the upstream splicing branch point attacks the downstream 5' splice site, and the newly generated 3'-hydroxyl end of the circularizing exon attacks the upstream 3' splice site, releasing a circular exon. This process is catalyzed by the canonical machinery that carries out splicing, although the efficiency is lower (45). A substantial fraction of spliced transcripts gives rise to circRNAs, but the repertoire of transcripts from which circRNAs are derived is cell type-specific, supporting the notion that circRNA biogenesis and function may be highly regulated (46–48).

CircRNAs are believed to influence several cellular processes. The first molecular function identified for circRNAs is one of sequestration of microRNAs to modulate their availability to target mRNAs. The circRNA *CiRS-7* was found to contain multiple miR-7 binding sites and thus regulated miR-7 activity on target mRNAs (49,50). This inhibition led to increased myocardial infarction, by causing up-regulated expression of PARP and SP1 in myocardial cells, as both *PARP* and *SP1* mRNAs bear miR-7a target sites

(51). *SRY*, a circRNA expressed in murine testis, encompasses 16 binding sites for miR-138 and sponges this microRNA (49). Other examples include *CircHIPK3*, which binds to and sequesters miR-124 (52), and microRNAs in the miR-2284 family, which bind to circRNAs from cattle casein (*CSN*) genes (53).

Here, we used high-throughput RNA sequencing (RNA-Seq) to survey senescence-associated circRNAs (which we termed 'SAC-RNAs') differentially expressed in proliferating (early-passage) and in senescent (late-passage) human diploid WI-38 fibroblasts. Among the circRNAs selectively reduced in senescent cells, we focused on *CircPVT1*, a moderately expressed circRNA generated by circularization of an exon of the *PVT1* pre-lncRNA, as silencing *CircPVT1* in proliferating cells triggered senescence. Several microRNAs were predicted to bind *CircPVT1*, but only let-7 was found enriched in endogenous *CircPVT1* pulled down from cells, suggesting that *CircPVT1* might modulate let-7 activity and influence expression of downstream targets. After obtaining evidence that *CircPVT1* decreased the cellular pool of available let-7, we found that silencing *CircPVT1* rescued the proliferative phenotype caused by antagonizing let-7. Moreover, several let-7 target mRNAs encoding proliferative proteins that prevent senescence were suppressed by silencing *CircPVT1* levels, particularly IGF2BP1, KRAS and HMGA2. In sum, we have found that the senescence-associated circRNA *CircPVT1* binds to let-7 and inhibits its actions and thereby influences senescence.

MATERIALS AND METHODS

Cell culture, ionizing radiation (IR), siRNA transfection and SA- β -galactosidase activity

Human WI-38 fibroblasts, MCF7 breast carcinoma cells, and IMR-90 lung fibroblasts were cultured in Dulbecco's modified Eagle's medium (DMEM) supplemented with 10% fetal bovine serum (FBS), antibiotics, and non-essential amino acids (Invitrogen). Human breast epithelial MCF10a cells, lung epithelial BEAS-2B cells, and lung adenocarcinoma A549 cells were cultured in DMEM supplemented with 10% FBS and antibiotics. Human non-small cell lung carcinoma H1299 cells were cultured in Roswell Park Memorial Institute (RPMI) 1640 medium supplemented with 10% FBS and antibiotics. Proliferating WI-38 cells were used at population doublings (PDL) between 15 and 25, and senescent fibroblasts were used after additional culture, at PDLs 50–55. Proliferating WI-38 cells were exposed to ionizing radiation (10 Gy) and cultured for 10 days to induce senescence. Ctrl siRNA (AAUUCUCCGAACGUGUCACGU, Qiagen), anti-let-7 antagomir (AACUAUACAACCUACUACCUCA, Ambion), let-7 mimic (UGAGGUAGUAGGUUGUAUAGUU, Ambion), and *CircPVT1* siRNA (CUGUCAGCUGCAUGGAGCUUCGU, IDT) were transfected at 100 nM final concentration using Lipofectamine-2000 (Invitrogen). Senescence-associated (SA) β -galactosidase activity in WI-38 cells was assessed using a kit from Cell Signaling Technology.

Western blot analysis

Whole-cell lysates were prepared in RIPA buffer containing protease inhibitors and were separated by SDS-polyacrylamide gel electrophoresis (SDS-PAGE), and transferred onto nitrocellulose membranes (Invitrogen iBlot Stack). Incubations with primary antibodies recognizing KRAS (Abcam), IGF2BP1 (Proteintech), HMGA2 (Abcam), P21 (Millipore), TP53, GAPDH or HSP90 (Santa Cruz Biotech), were followed by incubations with the appropriate secondary antibodies conjugated with horseradish peroxidase (HRP; GE Healthcare). Signals were developed using Enhanced Chemiluminescence (ECL).

Antisense oligomer pulldown

For antisense oligomer pulldown of *CircPVT1*, WI-38 cells were lysed in polysome extraction buffer (PEB, 20 mM Tris-HCl at pH 7.5, 100 mM KCl, 5 mM MgCl₂ and 0.5% NP-40) with protease and RNase inhibitors for 10 min on ice and the supernatant was collected by centrifugation (15 000 × g, 10 min, 4°C). The lysates were incubated with 100 pmol of biotin-labeled control oligomers (GCTGGTAGAGGGAGCAGATG-bio) or an oligomer complementary to the junction sequence of *CircPVT1* (bio-GCCAAAAGATCAGGCCTCAAGCCCAGCTGA, also known as Biotin-ASO) in 1× TENT buffer (10 mM Tris-HCl at pH 8.0, 1 mM EDTA at pH 8.0, 250 mM NaCl, 0.5% [v/v] Triton X-100) containing protease and RNase inhibitors for 1 h at 25°C with rotation. Streptavidin-coupled Dynabeads (50 µl, Invitrogen), were washed with 1× TENT buffer and incubated with lysate (30 min, 25°C, rotation). After isolating and washing the beads three times with ice-cold 1× TENT buffer, RNA was isolated using TRIzol, and *CircPVT1* and associated microRNAs in the pulldown were detected by RT-qPCR analysis.

RNA isolation and RT-qPCR analysis

RNA was isolated from WI-38 cells or from pulldown samples using TRIzol (Thermo Fisher Scientific) following the manufacturer's procedure. Total RNA was used for gene expression analysis by reverse transcription (RT) followed by quantitative (q)PCR analysis. RT was performed by using random hexamers and reverse transcriptase (Maxima Reverse Transcriptase, Fermentas) and qPCR was carried out using gene-specific primers and SYBR green master mix (Kapa Biosystems) in Applied Biosystems 7300 and 7900 instrument, as described (54). The relative expression levels of circRNAs were calculated using the primers listed in Supplementary Table S1 and the $2^{-\Delta\Delta CT}$ method using *18S* rRNA, *GAPDH* mRNA or *ACTB* mRNA for normalization (55). Student's t-test was used for assessing significance (*P*-values).

Ribonucleoprotein immunoprecipitation (RIP) analysis

The association of *CircPVT1* with endogenous RNA-binding proteins (RBPs) present in WI-38 fibroblasts was analyzed by ribonucleoprotein (RNP) immunoprecipitation (IP) as described (54). Briefly, proliferating WI-38 cells

were lysed in polysome extraction buffer (PEB; 20 mM Tris-HCl at pH 7.5, 100 mM KCl, 5 mM MgCl₂ and 0.5% NP-40) supplemented with RNase and protease inhibitors. The cytoplasmic lysates were incubated with protein A sepharose beads coated with antibodies recognizing DGCR8, HNRNPA1, KHSRP, LIN28 (Abcam) or control IgG (Santa Cruz Biotech) for 2 h at 4°C with rotation. Following washes with ice-cold NT2 buffer (50 mM Tris-HCl [pH 7.5], 150 mM NaCl, 1 mM MgCl₂, 0.05% NP-40), the RNA bound to the RNP complexes was isolated using TRIzol and used for RT-qPCR analysis.

Circular RNA sequencing and annotation

After isolation of total RNA using TRIzol (Invitrogen) and assessment of quality and quantity using the Agilent 2100-Bioanalyzer, ribosomal RNA was removed by rRNA Depletion Nano kit (Qiagen) and cDNA was prepared and amplified using the Ovation RNA-Seq System V2 (NuGEN) kit following the manufacturer's instructions. The amplified cDNA was fragmented using a Bioruptor (Diagenode), adaptors were ligated to cDNA using TruSeq ChIP Sample Preparation kit (Illumina, San Diego, CA, USA), the DNA fragments were size-selected (300–350 bp) after electrophoresis on a 2.5% agarose gel, and the selected DNA was subjected to 17 cycles of PCR amplification. Library quality was determined on the Bioanalyzer 2100 and the final libraries were sequenced using the Illumina HiSeq 2500 instrument. Data are available at GSE85771.

For circRNA-Seq analysis, adapter contamination was removed from the raw FASTQ files and sequences were aligned to the human genome (hg19) with TopHat2 (v2.1.0), first to identify linear RNA and later to identify fusion transcripts using reads which did not align to the linear RNA. The program CIRCexplorer was run with the fusion transcripts obtained from TopHat2 using Ensembl GRCh37 Release 82 annotation to identify the circular RNAs (Supplementary Table S2). Additionally, the cleaned FASTQ files (after removing adapters) were used for finding circularizing junctions by employing the find_circ software. In short, the reads were aligned to linear RNA using Bowtie2 program and then the unmapped reads were split into two anchors and aligned using Bowtie2 followed by identification of circularizing junctions (Supplementary Table S3). Using CIRCexplorer and find_circ analysis, the combined circRNA junction read number from two proliferating and two senescent samples were normalized to the respective number of mapped reads and represented as 'reads per million'.

Plasmid constructs and reporter analysis

To prepare plasmid psiCHECK2-let-7, the let-7 antisense (AACTATAACAACCTACTACCTCA) sequence was cloned downstream of *renilla* ORF in psiCHECK2 vector. For reporter analyses, HeLa cells were transfected with Ctrl siRNA, CircPVT1 siRNA, anti-let-7 or let-7 mimic using Lipofectamine 2000, and 48 h later with 200 ng of psiCHECK2 and psiCHECK2-let-7 reporter plasmids. Sixteen hours after that, RL and FL activities were measured using Dual-Glo Luciferase Assay System (Promega).

Test of resistance to RNase R digestion and circRNA sequencing

Total RNA (2 µg) isolated from proliferating WI-38 cells was either left untreated (ctrl) or treated with 20 units of RNase R (RNR07250, Epicentre) in the presence of 1× RNase R buffer, 20 units of RiboLock RNase Inhibitor (Thermo Scientific), and incubated for 30 min at 37°C. The digested RNA was isolated using TRIzol, cDNA from the untreated and RNase R-treated RNA was prepared using maxima RT protocol (above), and 0.2 µl of the cDNA reaction was used as template for RT-qPCR analysis. The RT-qPCR product for *hsa_circ_PVT1_01* (*CircPVT1*) was resolved in ethidium bromide-stained, 2.5% agarose gels and visualized on an ultraviolet transilluminator. Forward and reverse primers (Supplementary Table S1) were used to sequence the amplified PCR products and identify the junction sequence.

RT-qPCR analysis of microRNAs

Total RNA from WI-38 fibroblasts or RNA from pulldown samples was extracted using TRIzol following the manufacturer's protocol. RNA samples were reverse-transcribed using the Mir-X™ microRNA First Strand Synthesis Kit (#638315, Clontech), microRNA-specific forward primer (Supplementary Table S1) and universal reverse primer were used to measure the levels of individual microRNAs by RT-qPCR analysis using Applied Biosystems 7300 and 7900HT instruments and normalized to *U6* RNA levels.

³H-Thymidine incorporation assays

Proliferating WI-38 fibroblasts were transfected with or without combinations of Ctrl siRNA, *CircPVT1* siRNA, anti-let-7 and let-7 mimic using Lipofectamine 2000; 3 days later, cells were treated with [methyl-³H]-Thymidine (NET027250UC, Perkin Elmer) for 16 h, whereupon cells were washed with PBS and collected. The incorporated radioactivity was measured using liquid scintillation counting, and the data were normalized to total protein amount.

Droplet digital PCR analysis

Droplet digital PCR analysis was used for quantification of the copy number of *CircPVT1* and lncRNA *PVT1* using cDNA synthesized from RNA isolated from proliferating WI-38 cells, as described above. A droplet PCR reaction (20 µl) was prepared using QX200™ ddPCR™ EvaGreen Supermix (#1864033, BIORAD, USA) containing 5 ng of cDNA and 250 nM of primers directed at *circPVT1* and lncRNA *PVT1*. A QX200™ automated droplet generator was used to generate PCR droplets. PCR amplification was conducted using a cycle setup of 5 min at 95°C and 40 cycles of 30 s at 95°C plus 60 s at 60°C, and signal stabilization for 5 min at 4°C with 5 min at 90°C.

RESULTS

Senescence-associated circRNAs (SAC-RNAs)

Compared with proliferating, early-passage [population doublings (PDLs) 15–25] WI-38 human diploid fibro-

lasts, senescent (PDLs 50 through 55) WI-38 fibroblasts displayed a flattened and enlarged morphology and increased senescence-associated β-galactosidase (SA-βgal) activity, a widely used senescence marker (56) (Figure 1A). Western blot analysis revealed higher levels of senescence markers such as CDKN1A/P21 and TP53 in senescent WI-38 cells (Figure 1B). Similarly, reverse transcription (RT) followed by quantitative (q)PCR analysis revealed that the senescence markers *CDKN2A/P16* mRNA and *P21* mRNA were elevated in senescent cells (Figure 1C). To identify circRNAs in WI-38 fibroblasts, total RNA was isolated from two young and two senescent WI-38 populations, and circRNAs were identified by RNA-Seq as described (Materials and Methods, GEO accession number GSE85771). Many circRNAs were identified in proliferating and senescent WI-38 cells; a partial list of highly expressed circRNAs is shown (Figure 1D) and the full list of the circRNAs identified by the annotation algorithms 'CIRCexplorer' and 'find_circ' is provided (Supplementary Tables S2 and S3, respectively). CircRNA analysis using the CIRCexplorer and find_circ algorithms identified ~2, 200 shared circRNA junctions out of total ~15 000 circular RNAs (Figure 1E). These analysis programs identified large numbers of novel circRNAs and many of the known circRNAs with circBase IDs (Supplementary Tables S2 and S3) (57). More than 50% of the circRNAs identified in WI-38 cells were intronic circular RNAs (ciRNA) and others were exonic circular RNAs (circRNA) (Figure 1F).

A limited screen of circular RNAs identified by RNA-Seq was performed on proliferating and senescent WI-38 cells by RT-qPCR using specific divergent primers (Figure 2A). The PCR products were further assessed on agarose gels to confirm that a single DNA species was amplified in each case except *hsa_circ_EPB41L2_03*, where a larger band (~250 bp) was amplified along with the expected product, which could be a nonspecific product or another circRNA isoform (Supplementary Figure S1A). Interestingly, a few circRNAs were significantly upregulated or downregulated in senescent cells, suggesting a role for these circRNAs in regulating WI-38 senescence. Among them, the circRNA *hsa_circ_PVT1_01* was found to be one of the most downregulated circRNAs in senescent WI-38 cells. To further validate the association of circRNA expression with cellular senescence, we induced premature senescence by exposing proliferating WI-38 cells to ionizing radiation (IR). IR-treated cells were found to have higher SA-βgal activity and other markers of senescence (Figure 2B and data not shown). Most of the circRNAs showed consistent patterns of expression in replicative (Figure 2A) and IR-induced senescence (Figure 2C), including *hsa_circ_PVT1_01*, which was reduced in both instances.

CircPVT1 induces cell proliferation and suppresses senescence

The circRNA *hsa_circ_PVT1_01* (CircBase ID: *hsa_circ_0001821*) is a 410-nt long circRNA that originates from the long noncoding RNA plasmacytoma variant translocation (*PVT1*, NR_003367.3) transcript, and was thus termed *CircPVT1* (Supplementary Figure S1C and D). To validate the existence of *CircPVT1* and

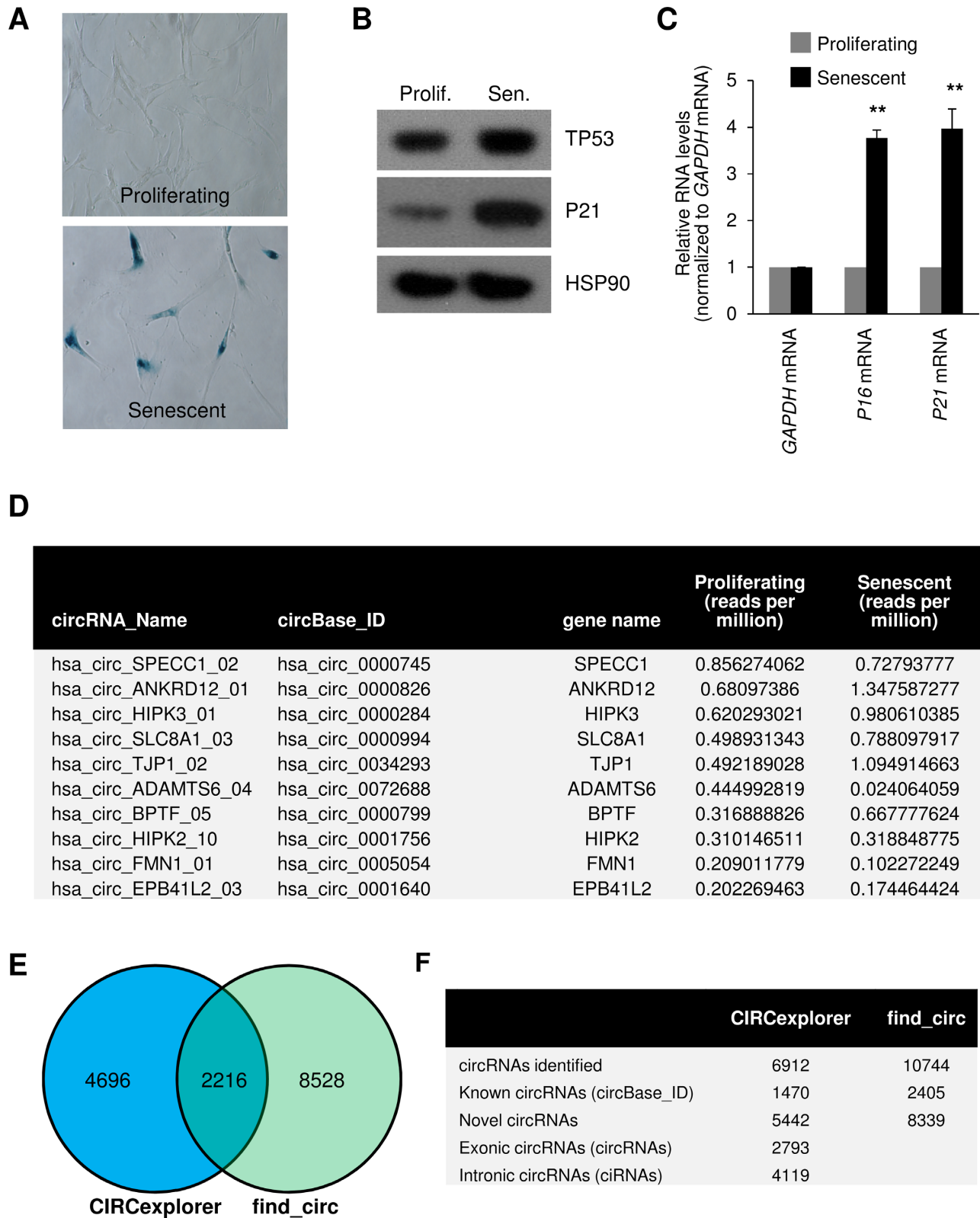


Figure 1. Identification and annotation of senescence-associated circRNAs in WI-38 fibroblasts. (A) Micrographs to visualize SA-β-gal activity in proliferating, early-passage, and senescent, late-passage WI-38 cells. (B) Western blot analysis of the levels of P53, P21, and loading control HSP90 in proliferating and senescent cells. (C) RT-qPCR analysis of the levels of *P16* mRNA, *P21* mRNA, and loading control *GAPDH* mRNA in proliferating and senescent cells. (D) Table of highly expressed circRNAs in proliferating WI-38 cells. (E) Venn diagram depicting the overlap between the two different circRNA prediction algorithms. (F) Number of circRNAs identified by the CIRCexplorer and find_circ algorithms. Data in (C) represent the means ± S.E.M. from three independent experiments. ***P* < 0.01 (Student's *t*-test).

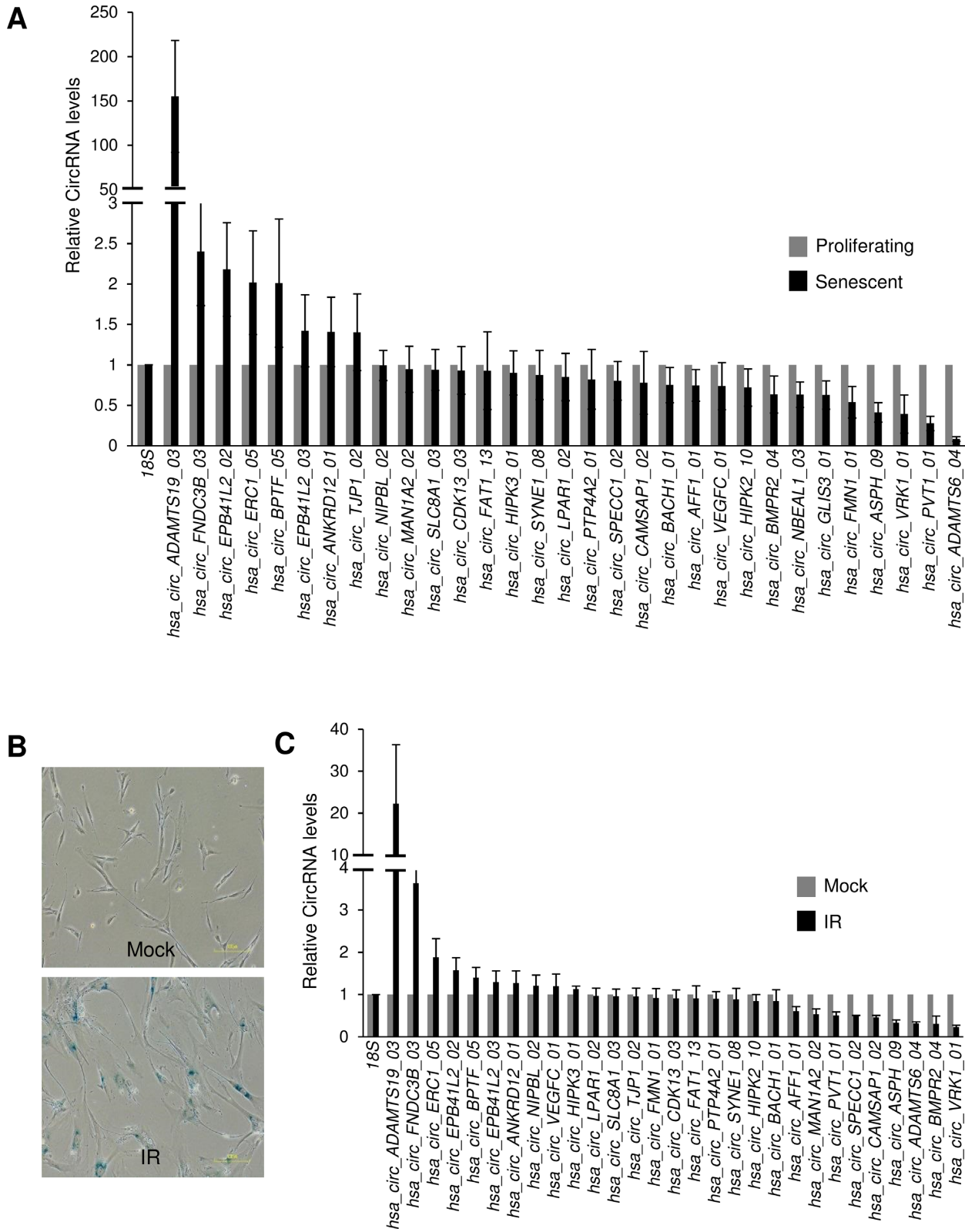


Figure 2. Characterization of senescence-associated circRNAs in WI-38 fibroblasts. **(A)** RT-qPCR analysis of changes in circRNA expression in proliferating and senescent WI-38 cells. **(B)** Representative images of SA- β gal staining in mock-treated and IR-treated (senescent) WI-38 cells. **(C)** RT-qPCR analysis of circRNA levels in mock-treated and IR-treated (senescent) WI-38 cells. Data in A and C are the means \pm S.E.M. from three independent experiments.

other SAC-RNAs, total RNA from proliferating WI-38 cells was treated with RNase R, which degrades the linear RNA without affecting the covalently circularized *CircPVTI*, and the levels of linear and circular RNAs in WI-38 cells were measured by RT-qPCR analysis using primers designed in a divergent orientation for the circular RNAs (Figure 3A). The *CircPVTI* PCR product was assessed on agarose gels to confirm that a specific circRNA species was amplified (Figure 3B), and the amplified PCR product was verified by DNA sequencing to confirm the amplification of the specific circRNA junction (Figure 3C). Droplet PCR analysis revealed that ~50 copies of *CircPVTI* are expressed per ng of WI-38 total RNA, while lncRNA *PVTI* is expressed at a higher level of ~200 copies per ng RNA (Figure 3D).

When comparing proliferating and senescent cells, the level of *PVTI* lncRNA did not change as significantly as did *CircPVTI*, suggesting that the levels of linear and circular *PVTI* transcript were regulated independently during cellular senescence (Supplementary Figure S1B). To further investigate the role of this circRNA in cell senescence, we silenced *CircPVTI* in WI-38 cells using an siRNA that lowered *CircPVTI* levels without affecting *PVTI* lncRNA levels (Figure 3E) (Materials and Methods). Silencing *CircPVTI* led to increased levels of senescence marker TP53 (p53) and triggered a flattened and enlarged cell morphology accompanied by increased SA- β gal activity (Figure 3F and G). Together, our results show that *CircPVTI* is expressed in proliferating WI-38 cells and suppressed cellular senescence. Given this evidence, we set out to investigate how *CircPVTI* might regulate the senescent phenotype.

Sponging of let-7 by *CircPVTI* prevents senescence

CircRNAs can enhance or suppress gene expression by modulating the availability of microRNAs for target mRNAs in the cell (49,50). As circRNAs have been shown to be highly stable, we hypothesized that *CircPVTI* could potentially act as a 'sponge' or a 'decoy', inhibiting the activity of associated microRNAs. We examined the microRNAs predicted to target *CircPVTI* (Figure 4A, Supplementary Table S4) (58) and investigated if such predicted microRNAs interact with *CircPVTI* by pulling down endogenous *CircPVTI* using antisense biotinylated oligomers targeting the *CircPVTI* junction (Figure 4B and C). The specificity for the pulldown of *CircPVTI* by the biotinylated antisense oligomer was confirmed by RT-qPCR analysis in Figure 4C. As shown in Figure 4D, a few microRNAs were enriched in the *CircPVTI* pulldown sample compared with the control pulldown samples, supporting the existence of circRNA-microRNA complexes. One of the microRNAs, let-7, was found to be the most highly enriched microRNA in the *CircPVTI* pulldown (Figure 4D); moreover, among the four circRNAs most downregulated in senescent cells (Figure 2A), *CircPVTI* had the highest density of let-7 sites (not shown). This result confirmed the specific interaction of *CircPVTI* with let-7 in WI-38 cells. Given the implication of let-7 in growth arrest and cell senescence (17,26,59), we explored this interaction further.

We asked if *CircPVTI* might influence cell proliferation and senescence by modulating let-7 availability in the

cells. Four days after blocking let-7 activity by transfecting a let-7 antagomir (anti-let-7), the expression levels of *CDKN1A* mRNA (encoding the senescence marker P21) decreased, while silencing *CircPVTI* elevated *CDKN1A* mRNA expression (Figure 5A). Western blot analysis revealed that anti-let-7 downregulated both P21 and TP53 (Figure 5B). Importantly, silencing *CircPVTI*, which increases let-7 availability, significantly reversed this loss of P21 and TP53 expression observed with anti-let-7 alone (Figure 5B). SA- β gal activity was elevated in *CircPVTI*-silenced cells, while anti-let-7 had the opposite effect, reducing SA- β gal activity and increasing proliferation; importantly, the proliferative phenotype seen after antagonizing let-7 was rescued when *CircPVTI* was silenced (Figure 5C). Together with the finding that the steady-state levels of let-7 are not significantly changed in proliferating relative to senescent WI-38 cells (Figure 5D), these results suggest that *CircPVTI* functions as a negative regulator of let-7 and thus suppresses cellular senescence.

Considering that miRNA function can be regulated at multiple levels, we examined whether *CircPVTI* might have a role in the maturation of let-7. For this, we tested by ribonucleoprotein immunoprecipitation (RIP) analysis if *CircPVTI* was capable of associating with several RNA-binding proteins (RBPs) implicated in let-7 processing and maturation, including DGCR8, KHSRP, HNRNPA1, and LIN28. Most of these RBPs (except LIN28) did show modest interaction with *CircPVTI* (Supplementary Figure S3A). We then tested if *CircPVTI* influenced let-7 biogenesis in WI-38 cells using RT-qPCR strategies to distinguish pri-, pre- and mature let-7 (Supplementary Figure S3B). We found that silencing *CircPVTI* did not change significantly pri- or pre-let-7 levels (Supplementary Figure S3C), suggesting that *CircPVTI* did not affect let-7 transcription or early processing, but it did lower mature let-7 levels slightly. These findings indicate that *CircPVTI* does not suppress let-7 activity by preventing let-7 biosynthesis, and further support the notion that reduced *CircPVTI* enhances let-7 function as an inhibitor of cell proliferation.

By acting as a decoy for let-7, *CircPVTI* promotes cell proliferation

The let-7 family of microRNAs has been shown to hinder cell growth by suppressing the expression of proliferative proteins such as IGF2BP1, KRAS and HMGA2 (35,40,43). The interaction of *CircPVTI* with let-7 prompted us to investigate whether the levels of *CircPVTI* affected WI-38 proliferation by sponging or sequestering let-7. Initial evidence in support of this possibility was obtained from experiments examining the correlation between let-7 activity as a function of WI-38 growth. As shown in Figure 5E, inhibition of let-7 by transfection of anti-let-7 increased cell numbers, while silencing *CircPVTI* decreased cell numbers, supporting the hypothesis that *CircPVTI* promoted cell proliferation by blocking let-7 activity. Interestingly, silencing of *CircPVTI* in anti-let-7-transfected cells partially rescued cell proliferation. Likewise, silencing *CircPVTI* significantly reduced the incorporation of ³H-thymidine in dividing cells while anti-let-7 elevated the ³H-thymidine incorporation (Figure 5F), and transfection of both *Cir-*

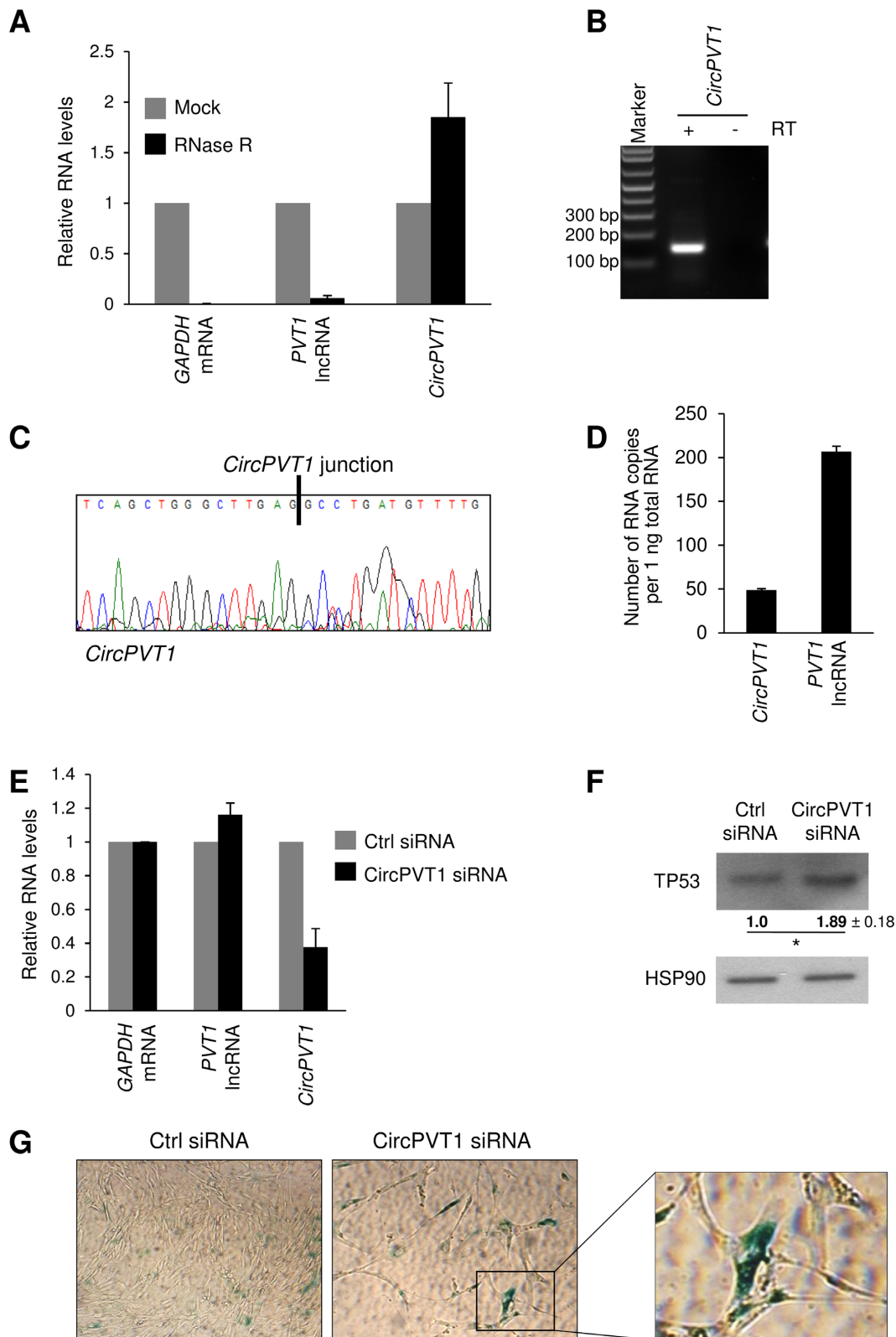


Figure 3. *CircPVT1* inhibits WI-38 cell senescence. (A) RT-qPCR results showing the abundance of circRNAs and linear RNAs in WI-38 cells treated with RNase R. The levels of *CircPVT1* and *PVT1* lncRNA were normalized to the values measured after mock treatments. (B) The RT-qPCR product of *CircPVT1* (\pm RT, with or without reverse transcription) was visualized by electrophoresis in ethidium bromide-stained 2.5% agarose gels. (C) qPCR products were purified and sequenced to confirm *CircPVT1* junction sequences. (D) Absolute quantification for *CircPVT1* and *PVT1* lncRNA in proliferating WI-38 cells. (E) RT-qPCR analysis of the levels of *CircPVT1* and *PVT1* lncRNA in proliferating WI-38 cells 4 days after transfection of Ctrl siRNA or *CircPVT1* siRNA. (F, G) Western blot analysis of the senescence marker TP53 (F) and SA- β gal staining (G) in WI-38 cells 4 days after transfection with Ctrl siRNA or *CircPVT1* siRNA. Data in A, D–F are the means \pm S.E.M. from three independent experiments. * $P < 0.05$ (Student's *t*-test).

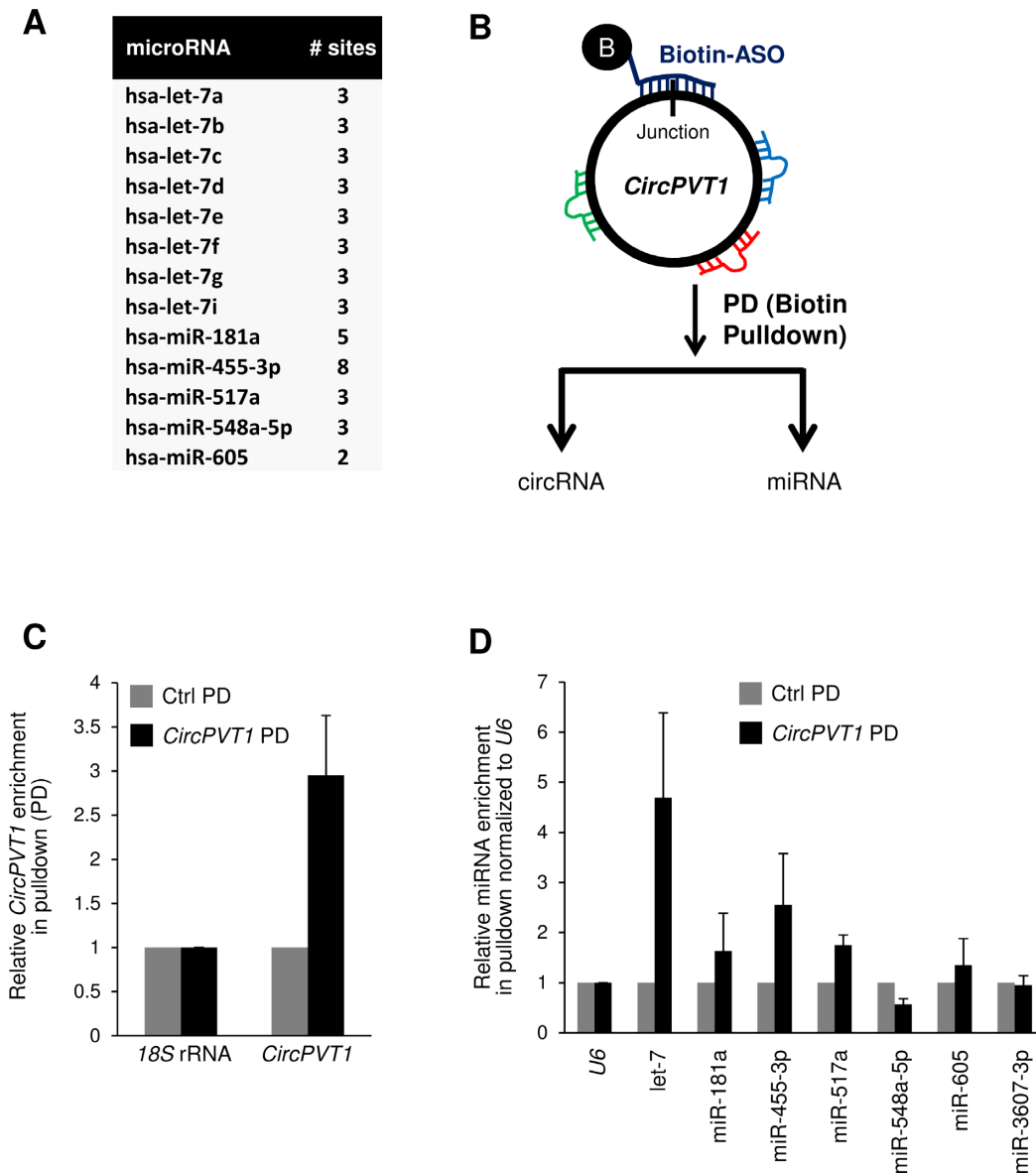


Figure 4. let-7 associates with *CircPVT1* in WI-38 cells. (A) List of microRNAs predicted to target *CircPVT1*. (B) Schematic of *CircPVT1* pulldown for specific detection of microRNAs associated with *CircPVT1* in WI-38 cells. (C) RT-qPCR analysis of the enrichment of *CircPVT1* in *CircPVT1* pulldown compared with control. (D) Enrichment of microRNAs predicted to target *CircPVT1* in *CircPVT1* pulldown analyzed by RT-qPCR. Data in (C, D) are the means \pm S.E.M. from at least three independent experiments.

cPVT1 siRNA and anti-let-7 rescued the reduction in ^3H -thymidine incorporation. Together, these results support the notion that *CircPVT1* controls the proliferation of WI-38 cells by modulating let-7 activity. Given that let-7 inhibits cell proliferation partly by inhibiting the production of IGF2BP1, KRAS, and HMGA2 (35,36,40,43), we hypothesized that *CircPVT1* might alter let-7 activity to promote WI-38 cell proliferation and inhibit cellular senescence.

To investigate whether *CircPVT1* influenced let-7 activity, we prepared luciferase reporter vectors derived from the parent plasmid psiCHECK2. A let-7 complementary sequence was cloned downstream of the renilla luciferase (RL) coding sequence, and firefly luciferase (FL) expressed

from the same construct served as internal normalization control (psiCHECK2-let-7, Figure 6A, top). Two days after transfecting HeLa cells with *CircPVT1* siRNA, anti-let-7 or pre-let-7, cells were transfected with the vector control (psiCHECK2) or with psiCHECK2-let-7. RL and FL activities were measured 16 h later and the ratio of RL activity to FL activity (RL/FL) was calculated. The RL/FL activity ratio in each population (control siRNA, *CircPVT1* siRNA) was assessed using the empty vector (psiCHECK2) as reference (Figure 6A). Although pre-let-7-transfected cells showed greater reduction in psiCHECK2-let-7 activity (RL/FL) (45% of control), silencing *CircPVT1* (Figure 6B) also significantly lowered RL/FL activity (70% of control),

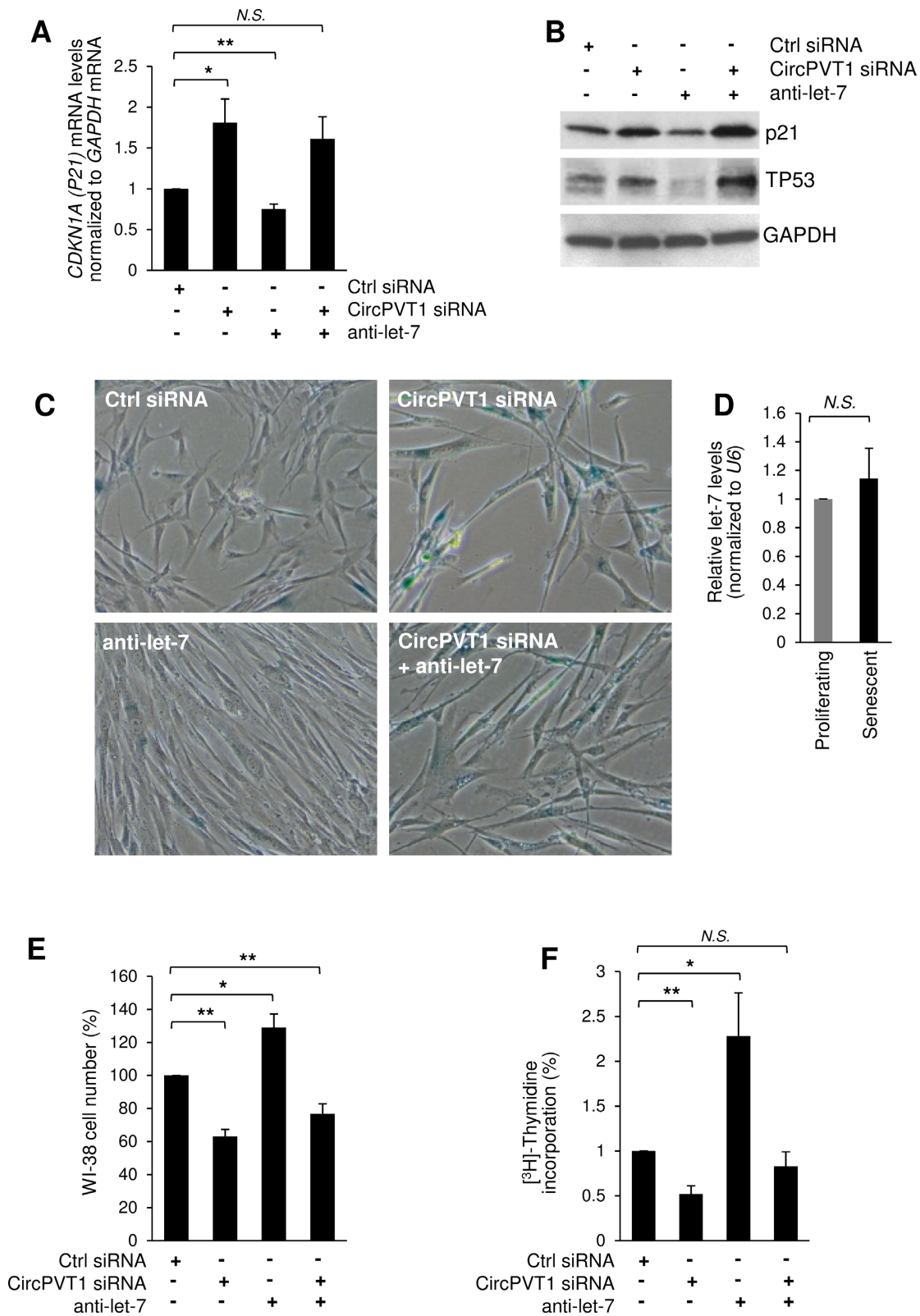


Figure 5. *CircPVT1* regulates cellular senescence by inhibiting let-7 function. (A) Proliferating WI-38 cells were transfected with *CircPVT1* siRNA or Ctrl siRNA, in the presence or absence of anti-let-7. The graph shows RT-qPCR measurements of the senescence marker *CDKN1A* (*P21*) mRNA in WI-38 cells 4 days after transfection with the two siRNAs above. N.S., not significant ($P = 0.06$); * $P < 0.05$; ** $P < 0.01$ (Student's *t*-test). (B) Western blot analysis of senescence marker P21, TP53, and loading control GAPDH in WI-38 cells 4 days after transfection with two siRNAs indicated. (C) SA- β gal staining in WI-38 cells 4 days after transfection with the siRNAs shown. (D) RT-qPCR analysis of let-7 levels in proliferating and senescent WI-38 cells. (E, F) Four days after transfection of WI-38 cells with the siRNAs indicated, cell numbers were counted (E) and measurements were taken for [³H]-thymidine incorporation (F). Data in A, D-F are the means \pm S.E.M. from three or four independent experiments. N.S., not significant; * $P < 0.05$; ** $P < 0.01$ (Student's *t*-test).

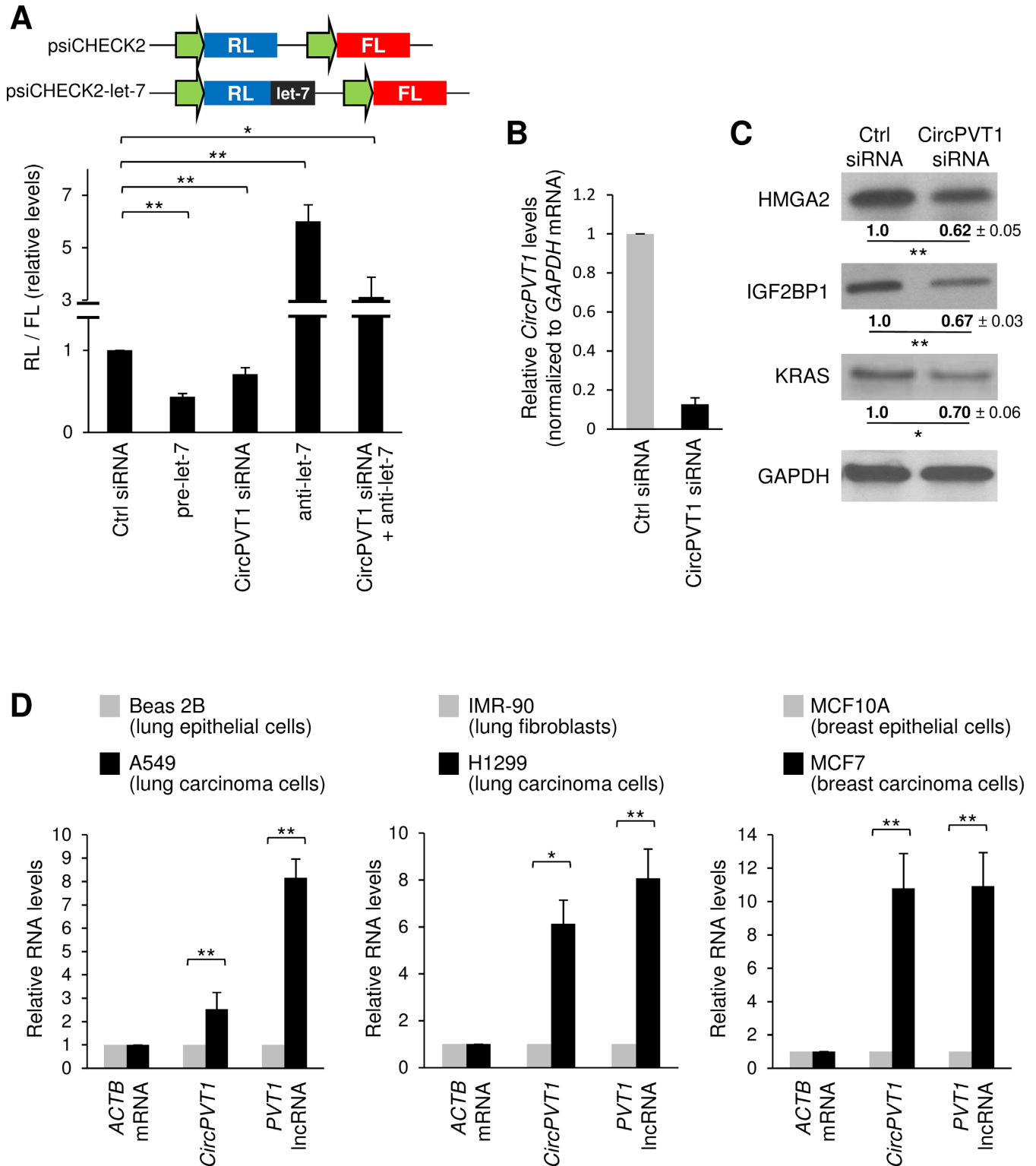


Figure 6. *CircPVT1* promotes translation of let-7 targets encoding proliferative proteins. (A) *Top*, schematic of the dual luciferase reporter plasmids derived from the parent vector psiCHECK2 (psi), which expresses renilla luciferase (RL) and the internal control firefly luciferase (FL), and psiCHECK2-derived plasmids bearing the target sequence of let-7. *Bottom*, 48 h after transfection of HeLa cells with *CircPVT1* siRNA, anti-let-7 or let-7 mimic, reporter plasmid was transfected, and 16 h later the ratio of RL activity to FL activity was measured. The changes in RL/FL ratios after the various small RNA transfections relative to RL/FL ratios of Ctrl siRNA-transfected cells are indicated. (B) RT-qPCR analysis of the levels of *CircPVT1* in proliferating WI-38 cells 4 days after transfection with Ctrl siRNA or *CircPVT1* siRNA. (C) Western blot analysis of the let-7 targets HMGA2, IGF2BP1, and KRAS, as well as loading control GAPDH in WI-38 cells 4 days after transfection with Ctrl siRNA or *CircPVT1* siRNA. (D) RT-qPCR analysis of the levels of *CircPVT1* and lncRNA *PVT1* in three sets of cancerous and noncancerous lines from lung [BEAS-2B versus A549 (*left*) and IMR-90 versus H1299 (*center*)] and breast [MCF10A vs MCF7 (*right*)]. *ACTB* mRNA was used as a normalization control. Data in A–D are the means ± S.E.M. from three independent experiments. **P* < 0.05; ***P* < 0.01 (Student's *t*-test).

indicating that *CircPVTI* reduced the availability of functional let-7 to transcripts bearing a let-7 site (Figure 6A).

Further validation of this hypothesis was sought by investigating if *CircPVTI* regulated the expression levels of let-7 targets IGF2BP1, KRAS and HMGA2. As shown in Figure 6C, expression of these proteins was consistently reduced after silencing *CircPVTI*, in agreement with the notion that silencing *CircPVTI* elevated the concentration of functional let-7 (Figure 6A) and led to the suppression of let-7-target mRNAs, including three that encoded proliferative proteins IGF2BP1, KRAS and HMGA2. Interestingly, silencing *CircPVTI* in HeLa cells increased significantly the association of let-7 with AGO2, the microRNA-binding RBP component of RISC, indicating that *CircPVTI* represses let-7 activity at least in part by reducing the availability of let-7 (Supplementary Figure S3D). Taken together, these results suggest that the SAC-RNA *CircPVTI* binds to and functionally inactivates let-7, in turn promoting the translation of IGF2BP1, KRAS and HMGA2 in WI-38 cells. Given that let-7 can also suppress tumor growth (20,25–31), we tested whether *CircPVTI* might be differentially expressed in cancer and non-cancer cells and further studied if lncRNA *PVTI* expression changed proportionately. Measurement of *CircPVTI* levels in three sets of cancerous and non-cancerous cell lines (Figure 6D) revealed that both *CircPVTI* and *PVTI* were higher in lung (A549, H1299) and breast (MCF7) carcinoma cell lines than in non-cancerous cell lines from lung (epithelial BEAS-2B cells and IMR-90 fibroblasts) and breast (MCF10A epithelial cells).

In summary, we propose that in proliferating cells, the relatively abundant *CircPVTI* sequesters let-7 from its target mRNAs in order to derepress production of proliferation proteins and impede senescence (Figure 7). Accordingly, the reduction in *CircPVTI* levels in senescence allows greater let-7 functional availability in the cell to repress the expression of the let-7-target mRNAs.

DISCUSSION

We have characterized a new function for a circular RNA derived from the *PVTI* gene, *CircPVTI*, on cellular senescence. The decrease in *CircPVTI* levels in senescent WI-38 human fibroblasts appeared to be functionally important because knockdown of *CircPVTI* alone promoted senescence (Figure 3). In order to elucidate the mechanism whereby *CircPVTI* elicited this effect, we investigated whether it interacted with any specific microRNAs. Among the candidate microRNAs that might potentially interact with *CircPVTI*, let-7 showed the highest enrichment in *CircPVTI* pulldown assays (Figure 4). Since let-7 plays a role in promoting senescence by repressing the production of proliferative genes (35,40,43), we investigated a potential function for *CircPVTI* as an inhibitor or sponge of let-7. We found that senescence and growth arrest triggered by silencing *CircPVTI* were rescued if let-7 was neutralized using an anti-let-7 antagomir (Figure 5). These results were consistent with *CircPVTI* modulating the level of functional let-7 in the cell, as revealed by studying a let-7 luciferase reporter. Three proteins encoded by let-7 targets, HMGA2, IGF2BP1 and KRAS, showed reduced levels when *Cir-*

cPVTI was silenced and thus more let-7 molecules were available to regulate these target transcripts. In sum, we have identified a novel role for *CircPVTI* in preventing senescence by binding to and inhibiting let-7.

CircPVTI is generated through backsplicing of the last exon of the gene that encodes for *PVTI*, a lncRNA that is upregulated in cancer cells (60). LncRNA *PVTI* knockdown reduced cell proliferation in ovarian and breast cancer cells (61) and in hepatocellular carcinoma (62). The genetic locus is in close proximity to the gene that encodes the oncoprotein MYC (63) and this proximity was identified as one of the mechanisms through which *PVTI* functions in controlling the stability of MYC protein (64). *PVTI* was also proposed to regulate carcinogenesis via the microRNAs that it encodes (reviewed in (65)). Whether lncRNA *PVTI* plays a role in senescence, as we propose for *CircPVTI* in the present study, is not known. Conversely, however, it is plausible that *CircPVTI* promotes proliferation in other cellular states such as cancer, just as it promotes proliferation in nontransformed cells (Figure 5). Although lncRNA *PVTI* has been proposed to sponge miR-200 (66), there is no report to-date that it may sponge let-7. It is possible that let-7 binding to *PVTI* may cause degradation of the lncRNA and thus binding is prevented by a secondary structure unique to the linear form of *PVTI*. It will be important to assess directly whether *PVTI* is regulated by let-7 or may instead sponge let-7 as does *CircPVTI*. Although in WI-38 fibroblasts *CircPVTI* was 7 or 8 times less abundant than *PVTI* (Figure 3D), the relative abundance of the two transcripts has not been assessed in other cell types or tissues. In addition, investigating whether production of the two molecules is coordinately regulated or whether *CircPVTI* biogenesis is independent of *PVTI* production is also warranted. *PVTI* levels did not change significantly in senescent relative to proliferating cells (Supplementary Figure S1B), indicating that *CircPVTI* levels may be regulated at the levels of circularization or turnover. Specific RBPs may play a role in these processes and their own abundance or activity might be modulated during senescence, independently of the levels of the parent transcript lncRNA *PVTI*. In sum, we propose that the linear and circular form of *PVTI* may work in the same direction to control cell proliferation, albeit potentially through different mechanisms.

CircRNAs have been known for more than two decades but did not draw much attention until recently, when their high abundance was revealed by transcriptome-wide RNA-sequencing and several circRNAs have been characterized as inhibitors of microRNAs and thus regulators of gene expression (49,50). The regulatory function stems from their ability to bind microRNAs by sequence complementarity and their high stability due to their covalent circle structure. Our pulldown and functional studies corroborated this function, as *CircPVTI* was capable of binding selectively to let-7 and inhibiting let-7 function, despite the computational prediction that other microRNAs might also bind. This selectivity may be explained by the fact that *CircPVTI* may form a specific secondary structure that makes other putative microRNA sites inaccessible to microRNAs. It is also possible that certain RBPs may bind *CircPVTI* and mask microRNA-recognition sequences. Additionally, some computationally predicted targets may simply not

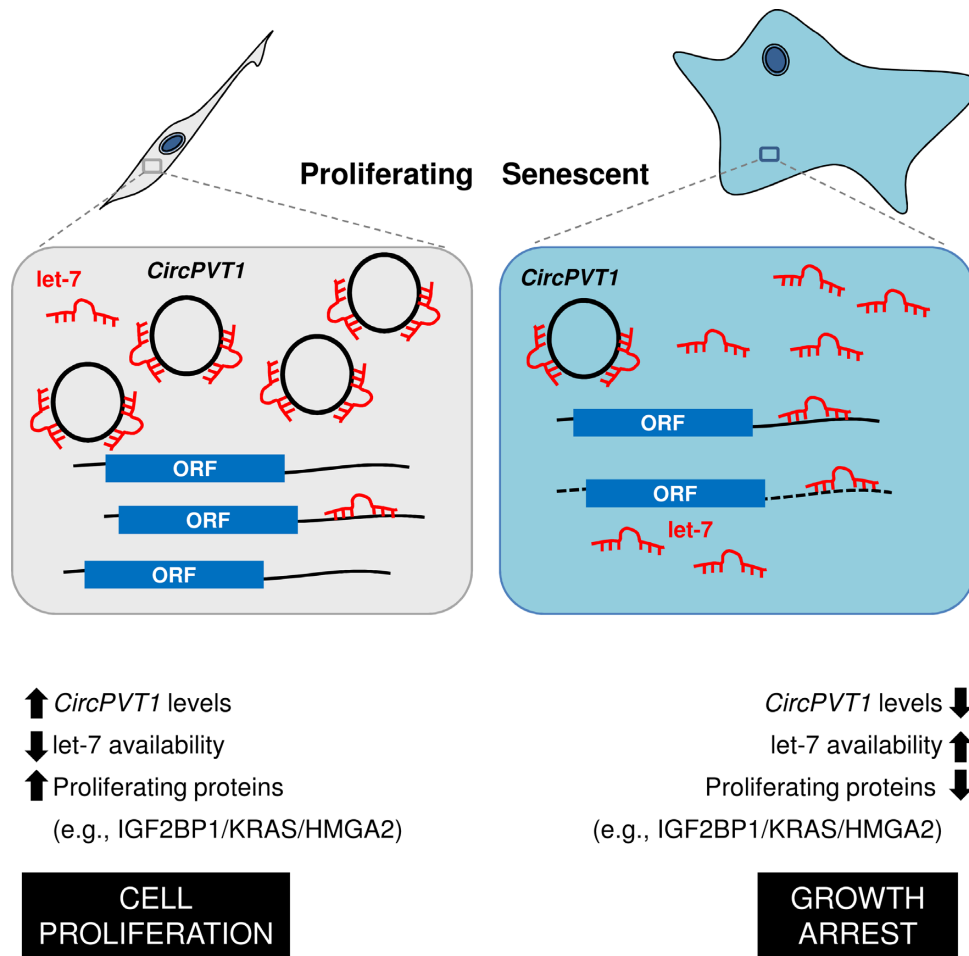


Figure 7. *CircPVT1* action model. Proposed model whereby *CircPVT1* acts as a competing endogenous RNA, sponging let-7; *CircPVT1* promotes the expression of target genes required for cell cycle progression by preventing let-7 from acting on such target mRNAs. The decreased expression levels of *CircPVT1* in senescent cells allows higher levels of functional let-7, which in turn suppresses let-7 target expression leading to growth inhibition and cellular senescence.

be expressed in WI-38 fibroblasts, and there are microRNAs that could potentially interact with *CircPVT1* but do not share standard sequence complementarity at the microRNA seed region.

Let-7 levels and activity have been shown to increase in senescent cells, and let-7 family members inhibit cell growth by suppressing the expression of target mRNAs encoding proliferative proteins (20,26,33,35). Like most microRNAs, let-7 can suppress gene expression by reducing the stability and/or translation of target mRNAs with which it shares partial complementarity. Given that *CircPVT1* can regulate let-7 activity generically and for a few target proteins (IGF2BP1, KRAS and HMGA2; Figure 6), we anticipate that *CircPVT1* might also modulate the levels of other let-7 targets, although such a global effect for *CircPVT1* remains to be investigated. It was somewhat surprising to find that an abundant microRNA such as let-7 [collectively comprising over 6,000 copies per cell (67)] could be sponged by a circRNA far less abundant (at ~5 copies per cell, with possibly three let-7 sites per molecule). However, given the vast number of let-7 target mRNAs, let-7-interacting RBPs [e.g. HuR, AUF1 and LIN28 (68,69)], and let-7 sponges [in-

cluding lncRNAs and mRNAs (67,70)], the number of let-7 molecules bioavailable to repress target transcripts is likely far smaller. The relative sponging of different members of the let-7 family (let-7a, -b, -c, -d, -e, -f, -g, -i, miR-98) by *CircPVT1* was not investigated, although let-7a is often the most abundant isoform. It was also interesting to find that *CircPVT1* did not influence early stages of let-7 biogenesis. The slight reduction in mature let-7 levels observed following *CircPVT1* silencing further solidifies the view that let-7 function and availability to target mRNAs increase when *CircPVT1* levels decline. Finally, we cannot exclude the possibility that other circular RNAs may regulate let-7 in a similar manner. However, among the circular RNAs that we tested for differential expression during senescence, *CircPVT1* had the highest density of let-7 sites (data not shown).

Like *CircPVT1*, a handful of other circRNAs have been found to sponge microRNAs (49–53,71). With rising evidence that some circRNAs can regulate gene expression programs, there is mounting interest in elucidating the mechanisms that generate circRNAs, the molecules with which they interact (RBPs, microRNAs and likely other

molecules as well), the mechanisms that control their sub-cellular localization, and more broadly, their impact on protein expression patterns, their cell and tissue function, and their influence on physiology and pathology. The discovery that *CircPVT1* promotes proliferation and prevents senescence paves the way for the analysis of other circRNAs that influence cell metabolism in different physiologic and disease states.

SUPPLEMENTARY DATA

Supplementary Data are available at NAR Online.

ACKNOWLEDGEMENTS

We thank the assistance of William H. Wood III (NIA) with experiments.

FUNDING

National Institute on Aging Intramural Research Program; National Institutes of Health (NIH). Funding for open access charge: National Institute on Aging, Intramural Research Program; NIH [Z01AG000393].

Conflict of interest statement. None declared.

REFERENCES

- Campisi, J. (2013) Aging, cellular senescence, and cancer. *Annu. Rev. Physiol.*, **75**, 685–705.
- Hayflick, L. (1965) The Limited in Vitro Lifetime of Human Diploid Cell Strains. *Exp. Cell Res.*, **37**, 614–636.
- Toussaint, O., Remacle, J., Dierick, J.F., Pascal, T., Fripiat, C., Royer, V., Magalhães, J.P., Zdanov, S. and Chainiaux, F. (2002) Stress-induced premature senescence: from biomarkers to likelihood of in vivo occurrence. *Biogerontology*, **3**, 13–17.
- Busuttill, R.A., Dolle, M., Campisi, J. and Vijg, J. (2004) Genomic instability, aging, and cellular senescence. *Ann. N. Y. Acad. Sci.*, **1019**, 245–255.
- Marcotte, R. and Wang, E. (2002) Replicative senescence revisited. *J. Gerontol. A Biol. Sci. Med. Sci.*, **57**, B257–B269.
- Campisi, J. and d'Adda di Fagnana, F. (2007) Cellular senescence: when bad things happen to good cells. *Nat. Rev. Mol. Cell. Biol.*, **8**, 729–740.
- Campisi, J. (2005) Senescent cells, tumor suppression, and organismal aging: good citizens, bad neighbors. *Cell*, **120**, 513–522.
- Ben-Porath, I. and Weinberg, R.A. (2005) The signals and pathways activating cellular senescence. *Intl. J. Biochem. Cell Biol.*, **37**, 961–976.
- de Magalhães, J.P., Chainiaux, F., de Longueville, F., Mainfroid, V., Migeot, V., Marcq, L., Remacle, J., Salmon, M. and Toussaint, O. (2004) Gene expression and regulation in H₂O₂-induced premature senescence of human foreskin fibroblasts expressing or not telomerase. *Exp. Gerontol.*, **39**, 1379–1389.
- van Deursen, J.M. (2014) The role of senescent cells in ageing. *Nature*, **509**, 439–446.
- Coppé, J.P., Desprez, P.Y., Krtolica, A. and Campisi, J. (2010) The senescence-associated secretory phenotype: the dark side of tumor suppression. *Annu. Rev. Pathol.*, **5**, 99–118.
- Tchkonia, T., Zhu, Y., van Deursen, J., Campisi, J. and Kirkland, J.L. (2013) Cellular senescence and the senescent secretory phenotype: therapeutic opportunities. *J. Clin. Invest.*, **123**, 966–972.
- Baker, D.J., Wijshake, T., Tchkonia, T., LeBrasseur, N.K., Childs, B.G., van de Sluis, B., Kirkland, J.L. and van Deursen, J.M. (2011) Clearance of p16^{Ink4a}-positive senescent cells delays ageing-associated disorders. *Nature* **479**, 232–236.
- Baker, D.J., Childs, B.G., Durik, M., Wijers, M.E., Sieben, C.J., Zhong, J., Saltness, R.A., Jeganathan, K.B., Verzosa, G.C., Pezeshki, A. et al. (2016) Naturally occurring p16^{Ink4a}-positive cells shorten healthy lifespan. *Nature* **530**, 184–189.
- Behm-Ansmant, I., Rehwinkel, J. and Izaurralde, E. (2006) MicroRNAs silence gene expression by repressing protein expression and/or by promoting mRNA decay. *Cold Spring Harb. Symp. Quant. Biol.*, **71**, 523–530.
- Abdelmohsen, K. and Gorospe, M. (2015) Noncoding RNA control of cellular senescence. *Wiley Interdiscipl. Rev. RNA*, **6**, 615–629.
- Maes, O.C., Sarojini, H. and Wang, E. (2009) Stepwise up-regulation of microRNA expression levels from replicating to reversible and irreversible growth arrest states in WI-38 human fibroblasts. *J. Cell Physiol.*, **221**, 109–119.
- Marasa, B.S., Srikantan, S., Martindale, J.L., Kim, M.M., Lee, E.K., Gorospe, M. and Abdelmohsen, K. (2010) MicroRNA profiling in human diploid fibroblasts uncovers miR-519 role in replicative senescence. *Aging*, **2**, 333–343.
- He, L., He, X., Lim, L.P., de Stanchina, E., Xuan, Z., Liang, Y., Xue, W., Zender, L., Magnus, J., Ridzon, D. et al. (2007) A microRNA component of the p53 tumour suppressor network. *Nature*, **447**, 1130–1134.
- Johnson, C.D., Esquela-Kerscher, A., Stefani, G., Byrom, M., Kelnar, K., Ovcharenko, D., Wilson, M., Wang, X., Shelton, J., Shingara, J. et al. (2007) The let-7 microRNA represses cell proliferation pathways in human cells. *Cancer Res.*, **67**, 7713–7722.
- Liu, Q., Fu, H., Sun, F., Zhang, H., Tie, Y., Zhu, J., Xing, R., Sun, Z. and Zheng, X. (2008) miR-16 family induces cell cycle arrest by regulating multiple cell cycle genes. *Nucleic Acids Res.*, **36**, 5391–5404.
- Sun, F., Fu, H., Liu, Q., Tie, Y., Zhu, J., Xing, R., Sun, Z. and Zheng, X. (2008) Downregulation of CCND1 and CDK6 by miR-34a induces cell cycle arrest. *FEBS Lett.*, **582**, 1564–1568.
- Ibanez-Ventoso, C., Yang, M., Guo, S., Robins, H., Padgett, R.W. and Driscoll, M. (2006) Modulated microRNA expression during adult lifespan in *Caenorhabditis elegans*. *Aging Cell*, **5**, 235–246.
- Reinhart, B.J., Slack, F.J., Basson, M., Pasquinelli, A.E., Bettinger, J.C., Rougvie, A.E., Horvitz, H.R. and Ruvkun, G. (2000) The 21-nucleotide let-7 RNA regulates developmental timing in *Caenorhabditis elegans*. *Nature*, **403**, 901–906.
- Calin, G.A., Sevignani, C., Dumitru, C.D., Hyslop, T., Noch, E., Yendamuri, S., Shimizu, M., Rattan, S., Bullrich, F., Negrini, M. et al. (2004) Human microRNA genes are frequently located at fragile sites and genomic regions involved in cancers. *Proc. Natl. Acad. Sci. U.S.A.*, **101**, 2999–3004.
- Boyerinas, B., Park, S.M., Hau, A., Murmann, A.E. and Peter, M.E. (2010) The role of let-7 in cell differentiation and cancer. *Endocr.-Relat. Cancer*, **17**, F19–F36.
- Takamizawa, J., Konishi, H., Yanagisawa, K., Tomida, S., Osada, H., Endoh, H., Harano, T., Yatabe, Y., Nagino, M., Nimura, Y. et al. (2004) Reduced expression of the let-7 microRNAs in human lung cancers in association with shortened postoperative survival. *Cancer Res.*, **64**, 3753–3756.
- Iorio, M.V., Ferracin, M., Liu, C.G., Veronesi, A., Spizzo, R., Sabbioni, S., Magri, E., Pedriali, M., Fabbri, M., Campiglio, M. et al. (2005) MicroRNA gene expression deregulation in human breast cancer. *Cancer Res.*, **65**, 7065–7070.
- Visone, R., Pallante, P., Vecchione, A., Cirombella, R., Ferracin, M., Ferraro, A., Volinia, S., Coluzzi, S., Leone, V., Borbone, E. et al. (2007) Specific microRNAs are downregulated in human thyroid anaplastic carcinomas. *Oncogene*, **26**, 7590–7595.
- Nadiminty, N., Tummala, R., Lou, W., Zhu, Y., Shi, X.B., Zou, J.X., Chen, H., Zhang, J., Chen, X., Luo, J. et al. (2012) MicroRNA let-7c is downregulated in prostate cancer and suppresses prostate cancer growth. *PLoS ONE*, **7**, e32832.
- Dahiya, N., Sherman-Baust, C.A., Wang, T.L., Davidson, B., Shih, Ie, M., Zhang, Y., Wood, W. 3rd, Becker, K.G. and Morin, P.J. (2008) MicroRNA expression and identification of putative miRNA targets in ovarian cancer. *PLoS ONE*, **3**, e2436.
- Jeong, H.C., Kim, E.K., Lee, J.H., Lee, J.M., Yoo, H.N. and Kim, J.K. (2011) Aberrant expression of let-7a miRNA in the blood of non-small cell lung cancer patients. *Mol. Med. Rep.*, **4**, 383–387.
- Tzatsos, A., Paskaleva, P., Lympieri, S., Contino, G., Stoykova, S., Chen, Z., Wong, K.K. and Bardeesy, N. (2011) Lysine-specific demethylase 2B (KDM2B)-let-7-enhancer of zester homolog 2 (EZH2) pathway regulates cell cycle progression and senescence in primary cells. *J. Biol. Chem.*, **286**, 33061–33069.
- Markowski, D.N., Helmke, B.M., Belge, G., Nimzyk, R., Bartnitzke, S., Deichert, U. and Bullerdiek, J. (2011) HMG2 and p14Arf: major

- roles in cellular senescence of fibroids and therapeutic implications. *Anticancer Res.*, **31**, 753–761.
35. Lee, Y.S. and Dutta, A. (2007) The tumor suppressor microRNA let-7 represses the HMGA2 oncogene. *Genes Dev.*, **21**, 1025–1030.
 36. Mayr, C., Hemann, M.T. and Bartel, D.P. (2007) Disrupting the pairing between let-7 and Hmga2 enhances oncogenic transformation. *Science*, **315**, 1576–1579.
 37. Fedele, M., Battista, S., Manfioletti, G., Croce, C.M., Giacotti, V. and Fusco, A. (2001) Role of the high mobility group A proteins in human lipomas. *Carcinogenesis*, **22**, 1583–1591.
 38. Zaidi, M.R., Okada, Y. and Chada, K.K. (2006) Misexpression of full-length HMGA2 induces benign mesenchymal tumors in mice. *Cancer Res.*, **66**, 7453–7459.
 39. Markowski, D.N., Winter, N., Meyer, F., von Ahsen, I., Wenk, H., Nolte, I. and Bullerdiek, J. (2011) p14Arf acts as an antagonist of HMGA2 in senescence of mesenchymal stem cells—implications for benign tumorigenesis. *Genes Chromosom. Cancer*, **50**, 489–498.
 40. Johnson, S.M., Grosshans, H., Shingara, J., Byrom, M., Jarvis, R., Cheng, A., Labourier, E., Reinert, K.L., Brown, D. and Slack, F.J. (2005) RAS is regulated by the let-7 microRNA family. *Cell*, **120**, 635–647.
 41. Chu, C.Y. and Rana, T.M. (2006) Translation repression in human cells by microRNA-induced gene silencing requires RCK/p54. *PLoS Biol.*, **4**, e210.
 42. Bell, J.L., Wachter, K., Muhleck, B., Pazaitis, N., Kohn, M., Lederer, M. and Huttelmaier, S. (2013) Insulin-like growth factor 2 mRNA-binding proteins (IGF2BPs): post-transcriptional drivers of cancer progression? *Cell. Mol. Life Sci.*, **70**, 2657–2675.
 43. Boyerinas, B., Park, S.M., Shomron, N., Hedegaard, M.M., Vinther, J., Andersen, J.S., Feig, C., Xu, J., Burge, C.B. and Peter, M.E. (2008) Identification of let-7-regulated oncofetal genes. *Cancer Res.*, **68**, 2587–2591.
 44. Jeck, W.R., Sorrentino, J.A., Wang, K., Slevin, M.K., Burd, C.E., Liu, J., Marzluff, W.F. and Sharpless, N.E. (2013) Circular RNAs are abundant, conserved, and associated with ALU repeats. *RNA*, **19**, 141–157.
 45. Zhang, Y., Xue, W., Li, X., Zhang, J., Chen, S., Zhang, J.L., Yang, L. and Chen, L.L. (2016) The biogenesis of Nascent circular RNAs. *Cell Rep.*, **15**, 611–624.
 46. Salzman, J. (2016) Circular RNA Expression: Its Potential Regulation and Function. *Trends Genet.*, **32**, 309–316.
 47. Chen, L.L. (2016) The biogenesis and emerging roles of circular RNAs. *Nat. Rev. Mol. Cell Biol.*, **17**, 205–211.
 48. Salzman, J., Chen, R.E., Olsen, M.N., Wang, P.L. and Brown, P.O. (2013) Cell-type specific features of circular RNA expression. *PLoS Genet.*, **9**, e1003777.
 49. Hansen, T.B., Jensen, T.I., Clausen, B.H., Bramsen, J.B., Finsen, B., Damgaard, C.K. and Kjems, J. (2013) Natural RNA circles function as efficient microRNA sponges. *Nature*, **495**, 384–388.
 50. Memczak, S., Jens, M., Elefsinioti, A., Torti, F., Krueger, J., Rybak, A., Maier, L., Mackowiak, S.D., Gregersen, L.H., Munschauer, M. et al. (2013) Circular RNAs are a large class of animal RNAs with regulatory potency. *Nature*, **495**, 333–338.
 51. Geng, H.H., Li, R., Su, Y.M., Xiao, J., Pan, M., Cai, X.X. and Ji, X.P. (2016) The circular RNA Cdr1as promotes myocardial infarction by mediating the regulation of miR-7a on its target genes expression. *PLoS ONE*, **11**, e0151753.
 52. Zheng, Q., Bao, C., Guo, W., Li, S., Chen, J., Chen, B., Luo, Y., Lyu, D., Li, Y., Shi, G. et al. (2016) Circular RNA profiling reveals an abundant circHIPK3 that regulates cell growth by sponging multiple miRNAs. *Nat. Commun.*, **7**, 11215.
 53. Zhang, C., Wu, H., Wang, Y., Zhu, S., Liu, J., Fang, X. and Chen, H. (2016) Circular RNA of cattle casein genes are highly expressed in bovine mammary gland. *J. Dairy Sci.*, **99**, 4750–4760.
 54. Panda, A.C., Abdelmohsen, K., Martindale, J.L., Di Germanio, C., Yang, X., Grammatikakis, I., Noh, J.H., Zhang, Y., Lehmann, E., Dudekula, D.B. et al. (2016) Novel RNA-binding activity of MYF5 enhances Cnd1/Cyclin D1 mRNA translation during myogenesis. *Nucleic Acids Res.*, **44**, 2393–2408.
 55. Livak, K.J. and Schmittgen, T.D. (2001) Analysis of relative gene expression data using real-time quantitative PCR and the 2(-Delta Delta C(T)) Method. *Methods*, **25**, 402–408.
 56. Itahana, K., Campisi, J. and Dimri, G.P. (2007) Methods to detect biomarkers of cellular senescence: the senescence-associated beta-galactosidase assay. *Methods Mol. Biol.*, **371**, 21–31.
 57. Glazar, P., Papavasileiou, P. and Rajewsky, N. (2014) circBase: a database for circular RNAs. *RNA*, **20**, 1666–1670.
 58. Kertesz, M., Iovino, N., Unnerstall, U., Gaul, U. and Segal, E. (2007) The role of site accessibility in microRNA target recognition. *Nat. Genet.*, **39**, 1278–1284.
 59. Peng, C.H., Liu, J.H., Woung, L.C., Lin, T.J., Chiou, S.H., Tseng, P.C., Du, W.Y., Cheng, C.K., Hu, C.C., Chien, K.H. et al. (2012) MicroRNAs and cataracts: correlation among let-7 expression, age and the severity of lens opacity. *Br. J. Ophthalmol.*, **96**, 747–751.
 60. Colombo, T., Farina, L., Macino, G. and Paci, P. (2015) PVT1: a rising star among oncogenic long noncoding RNAs. *BioMed. Res. Int.*, **2015**, 304208.
 61. Guan, Y., Kuo, W.L., Stilwell, J.L., Takano, H., Lapuk, A.V., Fridlyand, J., Mao, J.H., Yu, M., Miller, M.A., Santos, J.L. et al. (2007) Amplification of PVT1 contributes to the pathophysiology of ovarian and breast cancer. *Clin. Cancer Res.*, **13**, 5745–5755.
 62. Wang, F., Yuan, J.H., Wang, S.B., Yang, F., Yuan, S.X., Ye, C., Yang, N., Zhou, W.P., Li, W.L., Li, W. et al. (2014) Oncofetal long noncoding RNA PVT1 promotes proliferation and stem cell-like property of hepatocellular carcinoma cells by stabilizing NOP2. *Hepatology*, **60**, 1278–1290.
 63. Shtivelman, E. and Bishop, J.M. (1990) Effects of translocations on transcription from PVT. *Mol. Cell. Biol.*, **10**, 1835–1839.
 64. Tseng, Y.Y., Moriarity, B.S., Gong, W., Akiyama, R., Tiwari, A., Kawakami, H., Ronning, P., Reuland, B., Guenther, K., Beadnell, T.C. et al. (2014) PVT1 dependence in cancer with MYC copy-number increase. *Nature*, **512**, 82–86.
 65. Cui, M., You, L., Ren, X., Zhao, W., Liao, Q. and Zhao, Y. (2016) Long non-coding RNA PVT1 and cancer. *Biochem. Biophys. Res. Commun.*, **471**, 10–14.
 66. Paci, P., Colombo, T. and Farina, L. (2014) Computational analysis identifies a sponge interaction network between long non-coding RNAs and messenger RNAs in human breast cancer. *BMC Syst. Biol.*, **8**, 83.
 67. Powers, J.T., Tsanov, K.M., Pearson, D.S., Roels, F., Spina, C.S., Ebricht, R., Seligson, M., de Soysa, Y., Cahan, P., Theissen, J. et al. (2016) Multiple mechanisms disrupt the let-7 microRNA family in neuroblastoma. *Nature*, **535**, 246–251.
 68. Yoon, J.H., Abdelmohsen, K., Kim, J., Yang, X., Martindale, J.L., Tomimaga-Yamanaka, K., White, E.J., Orjalo, A.V., Rinn, J.L., Kreft, S.G. et al. (2013) Scaffold function of long non-coding RNA HOTAIR in protein ubiquitination. *Nat. Commun.*, **4**, 2939.
 69. Yoon, J.H., Jo, M.H., White, E.J., De, S., Hafner, M., Zucconi, B.E., Abdelmohsen, K., Martindale, J.L., Yang, X., Wood, W.H. 3rd et al. (2015) AUF1 promotes let-7b loading on Argonaute 2. *Genes Dev.*, **29**, 1599–604.
 70. Ghazal, S1, McKinnon, B2, Zhou, J3, Mueller, M4, Men, Y5, Yang, L6, Mueller, M2, Flannery, C1, Huang, Y7 and Taylor, HS7 (2015) H19 lncRNA alters stromal cell growth via IGF signaling in the endometrium of women with endometriosis. *EMBO Mol. Med.*, **7**, 996–1003.
 71. Xie, H., Ren, X., Xin, S., Lan, X., Lu, G., Lin, Y., Yang, S.S., Zeng, Z.C., Liao, W.T.L., Ding, YQ et al. (2016) Emerging roles of circRNA_001569 targeting miR-145 in the proliferation and invasion of colorectal cancer. *Oncotarget*, **7**, 26680–26691.